AMSE Association for the Advancement of Modelling & Simulation Techniques in Enterprises
IIETA International Information and Engineering Technology Association
Advancing the World of Information and Engineering

Modelling, Measurement and Control A
Vol. 91, No. 4, December, 2018, pp. 222-232
Journal homepage: http://iieta.org/Journals/MMC/MMC_A

Candid inquest on modeling methods of doubly fed induction generator, and corroboration through simulation study

K. Gayathri*, S. Jeevananthan

Department of Electrical and Electronics Engineering, Pondicherry Engineering College, Pondicherry, India

Corresponding Author Email: gayathri14_eee@pec.edu

https://doi.org/10.18280/mmc_a.910408

Received: 12 September 2018
Accepted: 15 December 2018

Keywords:
doubly fed induction generator (DFIG), synchronous rotating reference frame (SRRF), rotor reference frame (RRF), stator reference frame (SRF), transfer function (TF) model

ABSTRACT

The doubly fed induction generator (DFIG) based wind energy conversion system (WECS) is the ubiquitous system than its counterpart, the squirrel cage induction generator (SCIG), because of its attractive features such as the variable speed operation capability, the low operating noise, the mechanical stress mitigation, the flexible control over active and reactive power flows etc. Simulation studies on nascent WECSs necessitate the accurate and the restitution readied (for non-idealities) models of DFIG as inexact models will make past grave denouements in the stake. Generally, the modeling of electromagnetic machines can be realized as a differential equation (linear/non-linear) or a transfer function (Z/S domains) or in the state space form. Amid the host of DFIG models archived hitherto, there is neither a perennial nor a pristine model. This paper attempts to rekindle existing dynamic models of DFIG to assert the nuance in them, which will succor in culling the apposite model for nascent inquests, unequivocally. The tenet of each model is analyzed through mathematical equations and a comprehensive MATLAB 13 (Simulink-ode 23tb-solver) based simulation study. Comparison is on the basis of electromagnetic torque, rotor speed, rotor currents, real and reactive powers on stator and rotor side, etc.

1. INTRODUCTION

Nowadays, due to the impoverishing nature of fossil fuels and environmental concern about global warming, non-depleting renewable energy resources gaining more importance day by day all over the globe [1]. The renewable energy sources are hydro, solar, geothermal, wave, tidal, biomass and wind. Among these wind [2-3] is the most promising renewable energy technology till date, since it is the massive, indigenous, safe, clean power source and heavily dominated by onshore projects [4]. This technology had been established for power production, in the years nineteen eighties with few tens of kilowatts; eventually at the present days, the multi-megawatt range wind turbines are also being introduced for installation. Some [5] of the applications of wind energy are ship propulsion, grain cleaning, grinding grains, water pumping, windsurfing, kite flying and wind electric generation. The components of wind energy conversion system (WECS) involve two major part such as mechanical and electrical [6]. The mechanical section consists of rotor blades, hub, nacelle, tower, gearbox, speed sensor for wind, drive train, mechanical brakes, pitch and yaw drives. The process of converting the wind energy into mechanical energy is achieved through the airfoil-shaped rotor blades and the mechanical support is provided by the tower, nacelle and hubs, then with the assistance of the sensor [7] the wind direction as well as speed is measured. The yaw drive is employed to shift the blades of the rotor along with the nacelle in order to extract maximum power from the wind. The high torque low speed shaft of the wind turbine is coupled to the low torque high speed shaft of the electric generator through the gearbox. On the other hand, the electrical section consists of interface power electronic converter, electric generator [8], step-up transformer, and three phase collection point. The main purpose of electric generators is to transform the rotational mechanical power into electricity and the generator can be one amid [9-12], the induction generator (IG) are categorized as Squirrel Cage (SC), Wound Field (WF), Doubly fed (DF) and synchronous generator (SG) as Permanent Magnet (PM). Among this DFIG become the most popular in present wind power production system, because of its attractive features such as operating at variable speed, four quadrants running capability, and lower power losses compared to other generators. The function of power electronic converters (interfaces) is to convert variable voltage and frequency power from generator to fixed frequency and voltage power to grid.

The wind power generation system (WPGS) is a complicated system, which involves various parts such as wind turbine aerodynamics, drive train, electric generator, power electronic converter etc. Therefore, modeling of overall WPGS is a cumbersome task. Over several years, modeling of electromagnetic machines has been evolved tremendously. The foremost intention to the mathematical modeling in different approaches is to correlate electrical quantities of the machine (voltages and currents) with mechanical quantities of the machine (speed and torque). Among these parts, the main problematical system is electric generator; the intricacy is more even compared to respective motor mode, due to the presence of colossal dynamics and highly unpredictable operating situations. Therefore, detailed study on the modeling of the electric generator is mandate, in order to fulfill the overall requirements and to incorporate in particular application as well as to alleviate issues which may arise in

industries. Generally, the machine modeling can be realized in different approaches such as dynamic model, small/large signal model, transfer function model, state space model etc. In the dynamic model, the behavior of the system with respect to time is analyzed and represented by using differential equations; the small/large signal models are used to represent the non-linear system in terms of linear differential equation; the transfer function model (frequency domain approach) is also represented using differential equation, applicable only for time invariant system (TIVS) and it does not consider the initial conditions of the system. Finally, the state space model (time domain approach), which is valid for both TIVS and time variant system (TVS), considers a set of initial conditions of the system in an account. In transformer, for steady state and low frequency transient analysis T and π equivalent model was studied. In case of DC machine transfer function model were used for describing dynamic and steady state behavior of the system. In induction machine, mathematical models were developed based on the distributed and concentrated parameters. The distributed parameters cause high computation time and the model does not consider the influence of the temperature variation. On the other hand, the mathematical models with concentrated windings comprise different approaches such as the phase coordinate model and orthogonal direct-quadrature (dq) model obtained by axes transformation. The realization of real machine can be modeled in phase coordinate form. Depending on the rotor position the mutual stator to rotor inductances will vary accordingly which result in nonlinear model due to inherent magnetic coupling coefficient. It also complicates to understand the behavior of dynamic involved in the system. To understand the dynamic behavior of the system, in the year 1920s, orthogonal dq model has begun with R.H Park to represent the induction machine by eliminating the time varying inductance. This is done by transforming the balanced two phase (stator variables) orthogonal stationary system into synchronously rotating reference frame fixed at the rotor. In 1930s, H.C.Stanley has transformed the variables of rotor to a stationary reference frame fixed on the stator in order to eliminate the variable inductance with respect to time. Later, by transforming the variables of stator and rotor to an arbitrary reference frame, Krause and Thomas stated that the time varying inductance can be eliminated. Hence, representations of induction machine model in different axes have paved the way to view the machine in different way, which also enable the successful implementation of vector control (VC) concept to model the induction machine in different approach and it also valid for all types of AC machines. If all these model approaches are converted in terms of per unit description, to compare the behavior of any machine with different power ratings will become easier as all values are taken in same units. In the detailed model, several factors such as losses from friction and windage, skin effect, iron losses, magnetic saturation etc. are neglected that influence the behavior of the system. Though different approaches are available to model any machine, depending on the purpose the model can be modified appropriately in order to achieve specific objectives. Similarly, a kind of approach can also be possible to model the electric generator. Therefore, reviewing of different electromagnetic machine model is essential.

Generally, the equivalent circuit of DFIG is fifth order model, depending on the number of parameters and their physical significances, the order is decided. The elimination of stator flux dynamics [13] from the fifth order model that is the derivation of stator flux linkage of dq component has resulted in third order model. Further, by assuming the rotor speed as fixed, a second order model could be resulted. Therefore, as the order of the model decreases, the number of equivalent circuit parameter is pruned. In this model, currents of the rotor are mainly depended on the machine parameters such as mutual and stator inductance [14] and the deviation involved in these parameters may lead to inevitably deteriorated to the control accuracy of the stator current. Therefore, in order to trim down parameter dependence of stator current, a model in synchronous dq frame has been obtained by applying the Laplace transform [15]. Analytical field calculation method has been developed in [16] to calculate parameters and performances such as flux density in air gap, flux linkage and back electro motive force (BEMF) for the DFIG based on sub-domain technique. The effect of the iron loss mostly ignored in the machine model and vector controls, which influence the behavior of the stator currents, it lags with respect to voltage decreases. The paper [17] has addressed the DFIG model with the iron loss in order to mitigate losses inside the generator. To improve the theoretical prediction of the system in some cases both iron loss and magnetic saturation has been considered [18]. To achieve the decoupled control for real and reactive powers in this system [19], the stator field-oriented reference frame (dq) model was used, where the flux linkage of the stator is aligned along the direct axis component. During the balanced condition of DFIG, stator and rotor currents are maintained within the limit; the fault/unbalance condition leads to stator voltage drop and affects the flux linkages of stator and rotor. Therefore, to limit rotor currents the crowbar resistance has been introduced in [20]. The discrete time modeling is also called platform independent model mostly adopted for the application on any real time platform, computer or programmable devices such as digital signal processors (DSPs) or field programmable gate arrays (FPGAs) and to analyze this model paper [21] has used Tustin method and predictor corrector approximation method.

Although there are different models for the electric generator analysis, some are not appropriate to meet out the particular task since the system involves lot of dynamics and unpredictable operating situation. Therefore, understanding the purpose of each model is necessary; in order to modify the model further and to enhance performances of the system depend on the application. This paper discusses the performance of electromagnetic torque, rotor speed and currents, real and reactive powers on stator and rotor sides for DFIG system in both MATLAB-Simulink and mathematical approach.

2. DOUBLY FED INDUCTION GENERATOR (DFIG) AND TYPICAL APPLICATIONS

The DFIG is the most winsome and preferred choice for multi-megawatt range wind power generation due to its limberness in variable speed as well as the cost of the power electronics converter is low compared to other generators. Figure.1 shows the block schematic of DFIG based WECS. It consists of three phase windings on the rotor as well as on the stator, wind turbine, gear box, power electronic interface, transformer, three phase grid and controller. The three phase stator windings generate the stator magnetic field as it directly connected to the grid and the three phase rotor windings connected to the grid through the power electronic interface

which establishes the rotor magnetic field. The torque is generated due to the interaction of rotor and stator magnetic field. The stator flux is a function of grid frequency and voltage. The rotation based on the grid frequency match with the synchronous speed. Under the steady state condition, the grid voltage and stator flux are assumed to be constant. On the other hand, the fluxes of the rotor highly depend on current of rotor, which is controlled by the power electronic converter. Therefore, by controlling the angular position of the stator flux as well as the magnitude of the rotor current the torque is produced. Based on wind speed, the power electronic converter on the rotor side will operate at varying frequency, in order to regulate the output power of the DFIG the torque/speed/active power controller are used. The main purpose of the grid side converter is to regulate the voltage of the DC link capacitor which is coupled between the rotor side and grid side converter and also to control the exchange of active and reactive power.

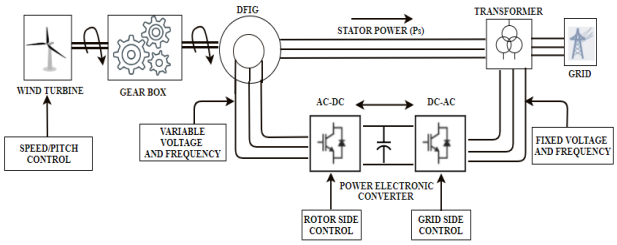

Figure 1. Block schematic of DFIG based WECS

2.1 Power flow in DFIG

The active power flow from the rotor circuit is bidirectional; therefore, either it injects/absorbs active power to the grid. To maximize the active power extraction (which depends on variable rotor speed) the power electronic converter arrangement is employed such that it allows a variable frequency operation. The active power injection/absorption depends on sub-synchronous and super-synchronous rotor speed which is the function of slip. At the synchronous speed, the magnetic field of the stator and the rotor will rotate at the same speed. Since the frequency of the grid and stator flux corresponds to synchronous speed. Therefore, no active power flow in the rotor windings and all the power will flow from the stator to the grid. Depend on the wind speed, the mechanical power (P_m) is delivered to the wind turbine and the correspondingly the rotor speed varies. Figure. 2(a), shows the active power flow representation under super synchronous speed (s<0). The super synchronous speed is obtained whenever the wind speed increases gradually the corresponding rotor speed increases above the synchronous speed and attain negative slip. In this mode, the active power is flows to the grid from both the windings stator and rotor. Figure. 2(b), shows the active power flow representation under sub synchronous speed (s>0). The sub synchronous speed is obtained whenever the wind speed decreases gradually the corresponding rotor speed also decreases below the synchronous speed and attains positive slip. In this mode, the active power is absorbed from the grid through the rotor windings.

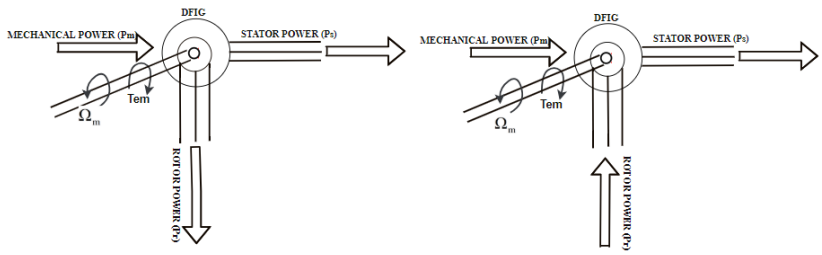

(a) Mode 1: Supersynchronous speed (s<0) (b) Mode 2: Subsynchronous speed (s>0)

Figure 2. Active power representations

3. REVIEW ON MODELING OF DFIG

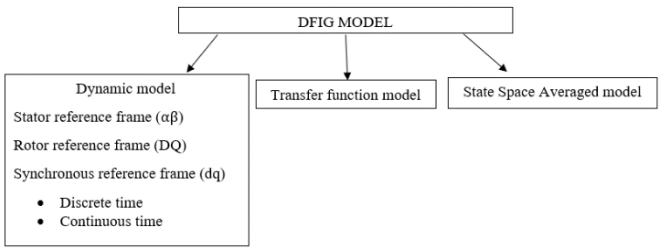

Figure 3. Realization of DFIG model

The foremost intention of this model is to study the dynamic behavior of the machine variables such as torque, currents, fluxes, dynamic oscillations and ripples under at steady state and transition periods. This model is represented using differential equation form. In order to derive the equivalent electric circuit, the three phase windings on stator and rotor are assumed as ideal. Under these conditions, the stator as well as rotor voltages, fluxes and currents of the machine are described. The mathematical modeling of DFIG can be realized as follows is shown in Figure. 3,

3.1 Dynamic model

The dynamic model of DFIG is developed by applying the space vector theory to the basic electric circuit. The space vector representation of reference frame is classified as stationary reference frame (αβ), rotor reference frame (DQ) and synchronous reference frame (dq) typically utilized to develop space vector-based model of DFIG. By using direct and inverse rotational transformations, a space vector can be represented in any of these frames.

3.1.1 Dq synchronously rotating reference frame model

In dq model, representing the synchronously rotating frame using space vector model, where both stator and the rotor equations multiplied by $e^{-j\theta s}$ and $e^{-j\theta r}$ respectively [22]. Figure.4 shows the model of DFIG in the dq reference frame. Figure.5 shows the flow chart for dq synchronously rotating reference frame model. The voltage equations in dq form are

as follows,

$$\vec{V}_s^a = R_s \vec{i}_s^a + \frac{d\vec{\psi}_s^a}{dt} + j\omega_s \vec{\psi}_s^a \;\; ; \vec{V}_r^a = R_r \vec{i}_r^a + \frac{d\vec{\psi}_r^a}{dt} + j\omega_r \vec{\psi}_r^a \quad (1)$$

Stator and rotor flux in dq form,

$$\begin{aligned} \psi_{ds} &= L_s i_{ds} + L_m i_{dr} \quad \psi_{dr} = L_r i_{dr} + L_m i_{ds} \\ \psi_{qs} &= L_s i_{qs} + L_m i_{qr} \; ; \; \psi_{qr} = L_r i_{qr} + L_m i_{qs} \end{aligned} \quad (2)$$

Stator and rotor active and reactive power in dq form,

$$\begin{aligned} P_s &= \frac{3}{2}(V_{ds} i_{ds} + V_{qs} i_{qs}) \;\; P_r = \frac{3}{2}(V_{dr} i_{dr} + V_{qr} i_{qr}) \\ Q_s &= \frac{3}{2}(V_{qs} i_{ds} - V_{ds} i_{qs}) \;\; Q_r = \frac{3}{2}(V_{qr} i_{dr} - V_{dr} i_{qr}) \end{aligned} \quad (3)$$

The electromagnetic torque expression,

$$T_{em} = \frac{3}{2} p(\psi_{qr} i_{dr} - \psi_{dr} i_{qr}) \quad (4)$$

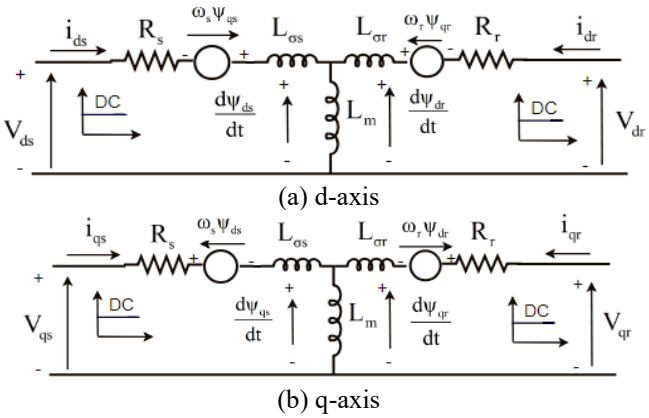

Figure 4. Model of DFIG synchronously rotating dq reference frame

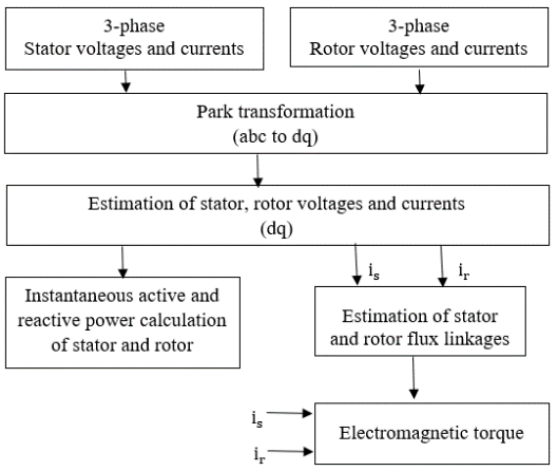

Figure 5. Flow chart for dq synchronously rotating reference model

In the general dq model, by transforming the three phase variables of stator and rotor into the rotating reference frame, the mutual inductance corresponds to stator and rotor become independent of rotor speed and position [23-24]. The voltages, currents and flux linkage expressions are similar but the electromagnetic torque is given as the function of flux linkage and currents with half of the pole pair. In [23], ω_e and T_e are used for angular frequency of stator and electromagnetic torque ω_s and instead T_{em}.

$$T_{em} = \frac{3}{2}\frac{p}{2}(\psi_{ds} i_{qs} - \psi_{qs} i_{ds}) \quad (5)$$

Similarly, the electromagnetic torque can also be expressed as follows. In [25], it has been expressed as the function of flux linkage and current with respect to stator along with mutual and stator inductance effects. With leakage inductances of stator and rotor as L_{ss}, L_n the electromagnetic torque, T_e is given as

$$T_{em} = \frac{3}{2}\frac{L_m}{L_s}(\psi_{qs} i_{ds} - \psi_{ds} i_{qs}) \quad (6)$$

The paper [26] has expressed the T_{em} as a function of stator and rotor currents with mutual inductance effect and represented the pole pair variable as N_p instead p and variable 'U' is used for representing the voltage equation on stator and rotor instead 'V'.

$$T_{em} = \frac{3}{2} N_p L_m (i_{dr} i_{qs} - i_{qr} i_{ds}) \quad (7)$$

In [27], T_{em} has been expressed as a function of flux linkage and current corresponding to the stator. φ symbol is used to represent flux linkage instead of ψ.

$$T_{em} = \psi_{ds} i_{qs} - \psi_{qs} i_{ds} \quad (8)$$

The three phase windings of the stator is coupled to the grid directly and three phase winding of rotor coupled to the grid through the power electronic interface therefore, whenever there is variation in the rotor current components, which will directly reflect the stator current as well as flux linkages [28]. In stator orientation, the reference frame is oriented with the stator flux linkage, V_{ds} becomes zero. From the dq synchronously rotating reference frame model (Figure. 5), the instantaneous power calculation of stator and rotor is modified by subtracting (V_{ds}=0). The modified power is obtained as the function of stator currents alone, and rotor currents with inductive effect as shown in Figure. 6. Modified power calculations with respect to stator and rotor currents. This model has represented the leakage inductances of stator and rotor as L_{ls} and L_{lr} respectively, which has also considered 'L_m' as the mutual inductance against the conventional assignment to the magnetizing inductance and ρ for differential (d/dt) operator.

Figure. 7 shows the simplified mathematical dq model help to analysis and also to predict the behavior of complex systems even at different operating conditions [29]. Where, the stator currents depend on rotor currents, by appropriately controlling

the rotor currents the active and reactive power exchange of the stator is controlled. This model has represented leakage inductances of stator and rotor as L_{ls}, L_{lr} instead $L_{\sigma s}$, $L_{\sigma r}$.

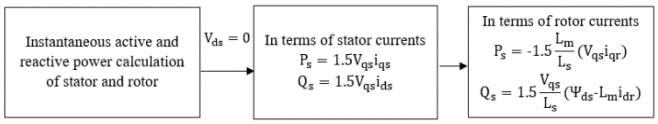

Figure 6. Modified power calculations in terms of stator and rotor currents

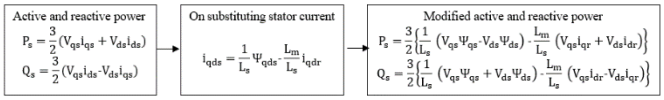

Figure 7. Modified power calculations

The control of stator flux orientation depends on the precision of stator resistance information and the value of stator resistance is usually very small [30]. In this model, the effect of stator resistance is neglected from the stator voltage equation as represented in Figure. 8.

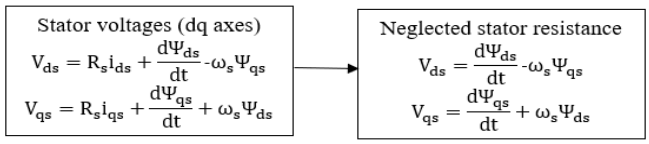

Figure 8. Neglected stator resistance

In this model, the stator flux transient is neglected, which would make the model unnecessarily complicated [31]. Neglecting the fast-varying terms is equivalent to neglect stator transients. In this reference frame, dq is revolving at synchronous speed, which means neglecting the d/dt (ψ_{ds}) term in the electrical equation of stator voltages. Therefore, elimination of two differential equations of the model is achieved, which also called third order model. The corresponding stator voltage electrical equations are modified as shown in Figure.9.

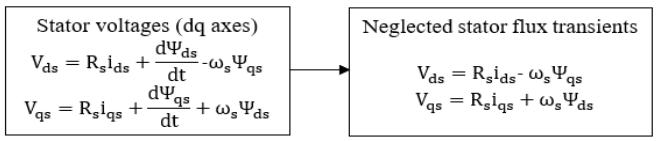

Figure 9. After omission of stator flux transient -$d\psi_{ds}/dt$

The rotor and stator resistance; leakage and mutual inductances are the most important parameters involved in DFIG impedance model [32]. Obviously, the parameter deviation likely occurs in stator and rotor resistance and leakage inductance. Among these, the leakage inductances play a more important task than the resistances. The magnetic saturation in DFIG system might happen as a result may vary the mutual inductance. In case of small and large scale systems, the mutual inductance (L_m) of the DFIG machine is much larger than the leakage inductance of the stator and the rotor ($L\sigma s$, $L\sigma r$). Therefore, in this model, the effect of mutual inductance is neglected. Figure. 10 shows the equivalent circuit with and without mutual inductance. This model has used the variable 'U' for representing the voltage equation on stator and rotor instead of 'V'.

Generally, in the standard d-q axis model, as mentioned in above discussion, neglects the variation in the main flux saturation and the existence of iron loss [33]. In order to enhance the hypothetical calculation and to scale back the error between calculated and measured values, this effect is considered into account.

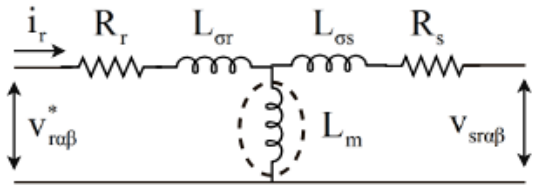

(a) With mutual inductance

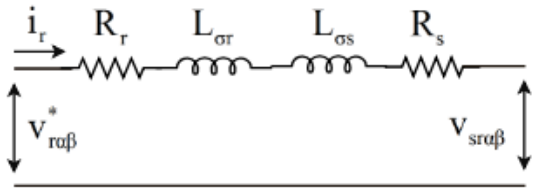

(b) Without mutual inductance

Figure 10. Equivalent circuit

3.1.2 αβ model

By using space vector theory, the three coils of stator and rotor of real machine can be represented as two phases stationary αβ coils for the stator and rotating coil DQ for the rotor. Figure. 11 shows the model of DFIG in the αβ reference frame [22]. Figure. 12 shows the flow chart for αβ stator reference frame model. The voltage equation of rotor must be multiplied by $e^{j\theta m}$, the corresponding voltage equations are as follows,

$$\vec{V}_s^s = R_s\vec{i}_s^s + \frac{d\vec{\psi}_s^s}{dt};\ \vec{V}_r^s = R_r\vec{i}_r^s + \frac{d\vec{\psi}_r^s}{dt} - j\omega_m\vec{\psi}_r^s \tag{9}$$

Stator and rotor fluxes in αβ form are,

$$\begin{aligned}\psi_{\alpha s} &= L_s i_{\alpha s} + L_m i_{\alpha s} \quad \psi_{\alpha r} = L_r i_{\alpha r} + L_m i_{\alpha r}\\ \psi_{\beta s} &= L_s i_{\beta s} + L_m i_{\beta s}\ ; \quad \psi_{\beta r} = L_r i_{\beta r} + L_m i_{\beta r}\end{aligned} \tag{10}$$

Real and reactive powers of stator and rotor are

$$\begin{aligned}P_s &= \frac{3}{2}(V_{\alpha s}i_{\alpha s} + V_{\beta s}i_{\beta s}) \quad P_r = \frac{3}{2}(V_{\alpha r}i_{\alpha r} + V_{\beta r}i_{\beta r})\\ Q_s &= \frac{3}{2}(V_{\beta s}i_{\alpha s} - V_{\alpha s}i_{\beta s}) \quad Q_r = \frac{3}{2}(V_{\beta r}i_{\alpha r} - V_{\alpha r}i_{\beta r})\end{aligned}\ ; \tag{11}$$

The electromagnetic torque can be expressed as,

$$T_{em} = \frac{3}{2}p(\psi_{\beta r}i_{\alpha r} - \psi_{\alpha r}i_{\beta r}) \tag{12}$$

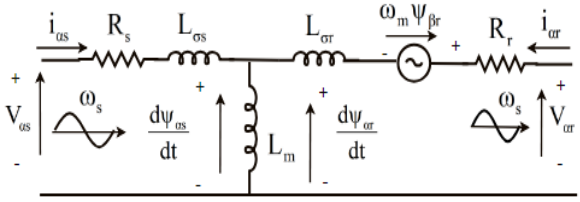

(a) Alpha-axis

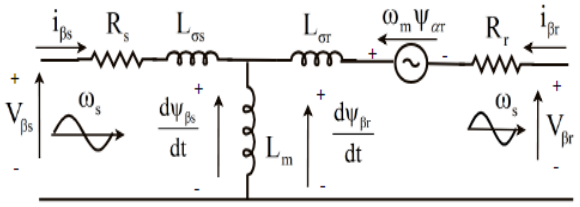

(b) Beta-axis

Figure 11. Model of DFIG in αβ reference frame

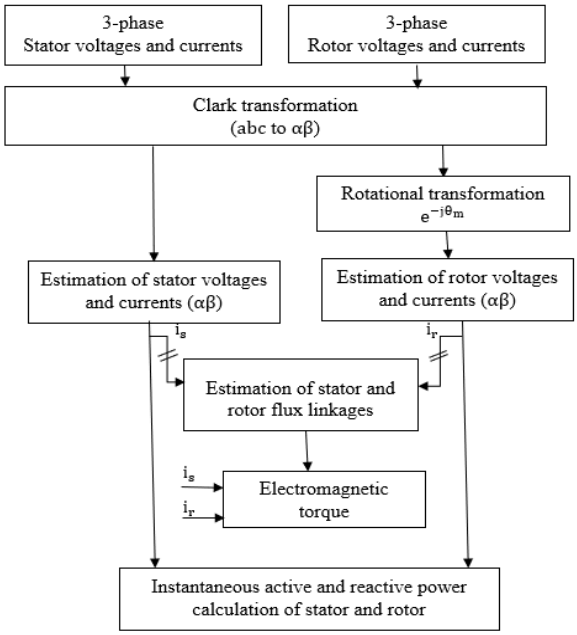

Figure 12. Flow chart for αβ stator reference frame model

Similarly, in this model, the estimated electromagnetic torque is also expressed as a function stator and rotor currents with mutual inductance effect.

$$T_{em} = \frac{3}{2} pL_m (i_{\alpha r} i_{\beta s} - i_{\alpha s} i_{\beta r}) \quad (13)$$

The instantaneous active power calculation of stator is shown in Figure.6, which is valid only under the balanced system [34]. Figure. 13 demonstrates the difference between traditional and extended active powers while Figure. 14 shows the flow chart derivation of extended active power from αβ model.

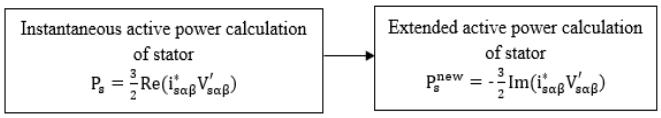

Figure 13. Difference between traditional and extended active powers

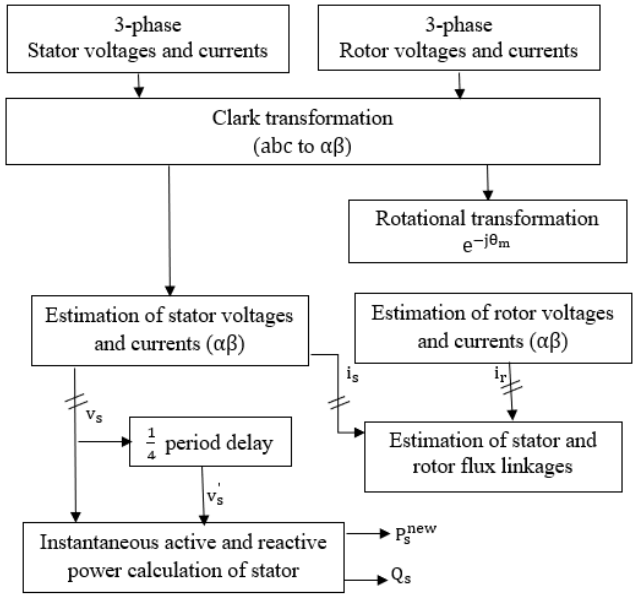

Figure 14. Flow chart derivation of extended active power from αβ model

When the system is unbalanced, there may be an existence of 3rd harmonic in the stator currents and electromagnetic torque oscillation, which is very harmful. Therefore, in this model, the extended active power calculation under unbalanced condition by introducing quarter of the fundamental period delay in $V_{\alpha\beta s}$ is performed. Therefore, $V_{s\alpha\beta}$ lags $V'_{s\alpha\beta}$. The obtained $V'_{s\alpha\beta}$ is used to find the extended active power.

3.1.3 Rotor reference frame

In dq rotor reference frame model, stator equations are multiplied by $e^{-j\theta r}$ [35]. Figure. 15 shows the flowchart for dq rotor reference frame model. Voltage equations in stator and rotor are as follows

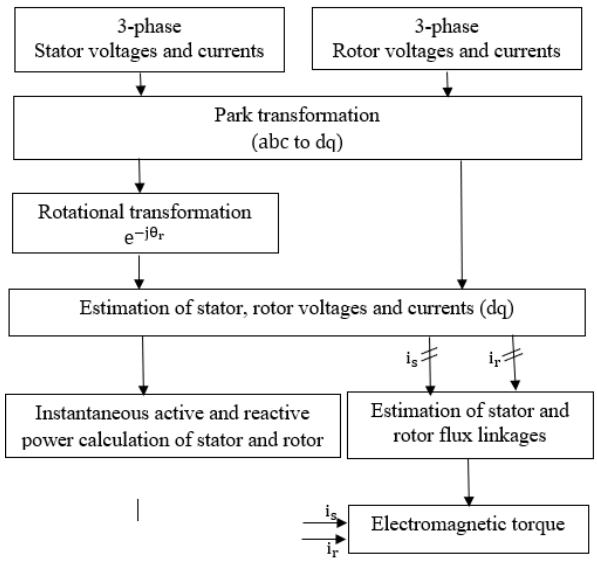

Figure 15. Flow chart for dq rotor reference frame model

$$V_{ds} = R_s i_{ds} + \frac{d\psi_{ds}}{dt} - \omega_r \psi_{qs} \quad ; \quad V_{qs} = R_s i_{qs} + \frac{d\psi_{qs}}{dt} + \omega_r \psi_{ds} \quad (14)$$

$$V_{dr} = R_r i_{dr} + \frac{d\psi_{dr}}{dt} \quad ; \quad V_{qr} = R_r i_{qr} + \frac{d\psi_{qr}}{dt} \tag{15}$$

The flux linkage, active and reactive power, electromagnetic torque equations are represented very similar to synchronously rotating dq reference frame DFIG model.

3.1.4 State space model

αβ Model in the stator coordinates equations are as follows [22], by using this model simulation is done.

$$\vec{v}_s^s = R_s \vec{i}_s^s + \frac{d\vec{\psi}_s^s}{dt}; \vec{v}_r^r = R_r \vec{i}_r^r + \frac{d\vec{\psi}_r^r}{dt} - j\omega_m \vec{\psi}_r^s \tag{16}$$

$$\vec{\psi}_s^s = L_s \vec{i}_s^s + L_m \vec{i}_r^s; \vec{\psi}_r^s = L_m \vec{i}_s^s + L_r \vec{i}_r^s \tag{17}$$

By using equations (16) and (17) considering fluxes as the state space magnitudes, the corresponding expressions are obtained as follows.

$$\frac{d}{dt}\begin{bmatrix}\vec{\psi}_s^s \\ \vec{\psi}_r^s\end{bmatrix} = \begin{bmatrix}\frac{-R_s}{\sigma L_s} & \frac{R_s L_m}{\sigma L_s L_r} \\ \frac{R_r L_m}{\sigma L_s L_r} & \frac{-R_r}{\sigma L_r} + j\omega_m\end{bmatrix}\begin{bmatrix}\vec{\psi}_s^s \\ \vec{\psi}_r^s\end{bmatrix} + \begin{bmatrix}\vec{v}_s^s \\ \vec{v}_r^s\end{bmatrix} \tag{18}$$

Expanding the equation (18), the expression of αβ components,

$$\frac{d}{dt}\begin{bmatrix}\psi_{\alpha s} \\ \psi_{\beta s} \\ \psi_{\alpha r} \\ \psi_{\beta r}\end{bmatrix} = \begin{bmatrix}\frac{-R_s}{\sigma L_s} & 0 & \frac{R_s L_m}{\sigma L_s L_r} & 0 \\ 0 & \frac{-R_s}{\sigma L_s} & 0 & \frac{R_s L_m}{\sigma L_s L_r} \\ \frac{R_r L_m}{\sigma L_s L_r} & 0 & \frac{-R_r}{\sigma L_r} & -\omega_m \\ 0 & \frac{R_r L_m}{\sigma L_s L_r} & \omega_m & \frac{-R_r}{\sigma L_r}\end{bmatrix}\begin{bmatrix}\psi_{\alpha s} \\ \psi_{\beta s} \\ \psi_{\alpha r} \\ \psi_{\beta r}\end{bmatrix} + \begin{bmatrix}v_{\alpha s} \\ v_{\beta s} \\ v_{\alpha r} \\ v_{\beta r}\end{bmatrix} \tag{19}$$

Currents as the state space magnitudes, expressions are as follows,

$$\frac{d}{dt}\begin{bmatrix}\vec{i}_s^s \\ \vec{i}_r^s\end{bmatrix} = \left(\frac{1}{\sigma L_s L_r}\right)\begin{bmatrix}-R_s L_r - j\omega_m L_m^2 & R_r L_m - j\omega_m L_m L_r \\ R_s L_m + j\omega_m L_m L_s & -R_r L_s + j\omega_m L_s L_r\end{bmatrix}\begin{bmatrix}\vec{i}_s^s \\ \vec{i}_r^s\end{bmatrix} + \left(\frac{1}{\sigma L_s L_r}\right)\begin{bmatrix}L_r & -L_m \\ -L_m & L_s\end{bmatrix}\begin{bmatrix}\vec{v}_s^s \\ \vec{v}_r^s\end{bmatrix} \tag{20}$$

Expanding the equation (20), the expression of αβ components,

$$\frac{d}{dt}\begin{bmatrix}i_{\alpha s} \\ i_{\beta s} \\ i_{\alpha r} \\ i_{\beta r}\end{bmatrix} = \begin{bmatrix}\frac{1}{\sigma L_s L_r}\end{bmatrix}$$

$$\begin{bmatrix}-R_s L_r & \omega_m L_m^2 & R_r L_m & \omega_m L_m L_r \\ -\omega_m L_m^2 & -R_s L_r & -\omega_m L_m L_r & R_r L_m \\ R_s L_m & -\omega_m L_m L_s & -R_r L_s & -\omega_m L_s L_r \\ \omega_m L_m L_s & R_s L_m & \omega_m L_r L_s & -R_r L_s\end{bmatrix}\begin{bmatrix}i_{\alpha s} \\ i_{\beta s} \\ i_{\alpha r} \\ i_{\beta r}\end{bmatrix}$$

$$\left(\frac{1}{\sigma L_s L_r}\right)\begin{bmatrix}L_r & 0 & -L_m & 0 \\ 0 & L_r & 0 & -L_m \\ -L_m & 0 & L_s & 0 \\ 0 & -L_m & 0 & L_s\end{bmatrix}\begin{bmatrix}v_{\alpha s} \\ v_{\beta s} \\ v_{\alpha r} \\ v_{\beta r}\end{bmatrix} \tag{21}$$

4. SIMULATION STUDY AND RESULTS

The main focus of this section is to compare mathematical (equation based) model and MATLAB-Simulink model of DFIG using MATLAB 13-Simulink tool (State space representation in αβ frame is subsumed). The performance of the system is compared in terms of the electromagnetic torque, the rotor speed, stator currents, rotor currents, the real power and the reactive power of both stator and rotor for the specification detailed in table 1.

Table 1. DFIG Parameters

Parameters	Values
Synchronous speed, (rpm)	1500
Rated power (MW)	2
Rated torque (kNm)	12.7
Rated stator voltage (V)	690
Pole pair, p	2
Rated rotor voltage (V)	2070
Turns ratio (u)	0.35
Ls, Lr (mΩ)	2.587
L_m (mΩ)	2.5
$L_{\sigma s}$, $L_{\sigma r}$ (mΩ)	0.087
R_s, R_r (Ω)	2.6

Figure 16 shows the simulation block diagram of DFIG, which arrives at inputs such as three phase stator voltages, three phase rotor voltages and the load torque from outputs such as three phase stator and rotor currents, two phase stationary stator and rotor fluxes, the electromagnetic torque and the rotor speed as functions of required electric and mechanical parameters such rotor and stator resistance, rotor, stator, magnetizing inductance, number of pole pairs and inertia.

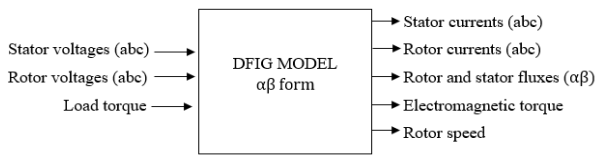

Figure 16. Simulation block diagram of DFIG

The above mentioned outputs can be calculated according to voltage inputs and corresponding machine parameters. By using the Clarke transformation, the three phase voltages are transformed in the stationary reference frame. By using this approach, the corresponding stator and rotor voltages, and currents in αβ components are calculated. Then with the help of the stator currents and rotor currents in αβ frame and machine parameters, the flux linkages of stator and rotor are calculated. Accordingly, the electromagnetic torque and the rotor speed are also calculated. Under the three different operating modes, sub-synchronous mode, synchronous mode and super-synchronous mode, the performance of the DFIG, in terms of real and reactive powers, the electromagnetic torque, the rotor speed, currents of stator and rotor, is discussed. The stator is always delivering the power to the grid under sub and super synchronous modes, and depending on whether the slip is positive or negative the rotor circuit or grid side converter can receive/deliver power from/to the grid. For both Simulink and mathematical models, the stator flux-oriented vector control is incorporated therefore, by controlling the rotor currents, the stator active and reactive powers as well as torque are well controlled. Figure.17. shows the comparison between the results (real power on stator and rotor) of MATLAB-Simulink and mathematical models. From the time 0 to 1.20 seconds the system operates in sub-synchronous mode (1217rpm), in which the generator operates below synchronous speed and the corresponding slip is positive (s=0.8). Therefore, the stator delivers real power (negative) to the grid while the rotor receives real power (positive) from the grid. Between the time 1.20 to 1.89 seconds the DFIG operates in synchronous speed (1500 rpm) and the corresponding slip is zero, only the stator delivers real power (negative) to the grid while the rotor neither receives nor deliver the real power. From the time 1.89 to 2.5 seconds the DFIG operates in super-synchronous speed (1800rpm), in which the generator operates above synchronous speed and the corresponding slip is negative (s=-0.2). Therefore, the both the stator and rotor deliver the real power (negative) to the grid. It is noted that whether the slip is positive or negative the DFIG is always operates in generating mode.

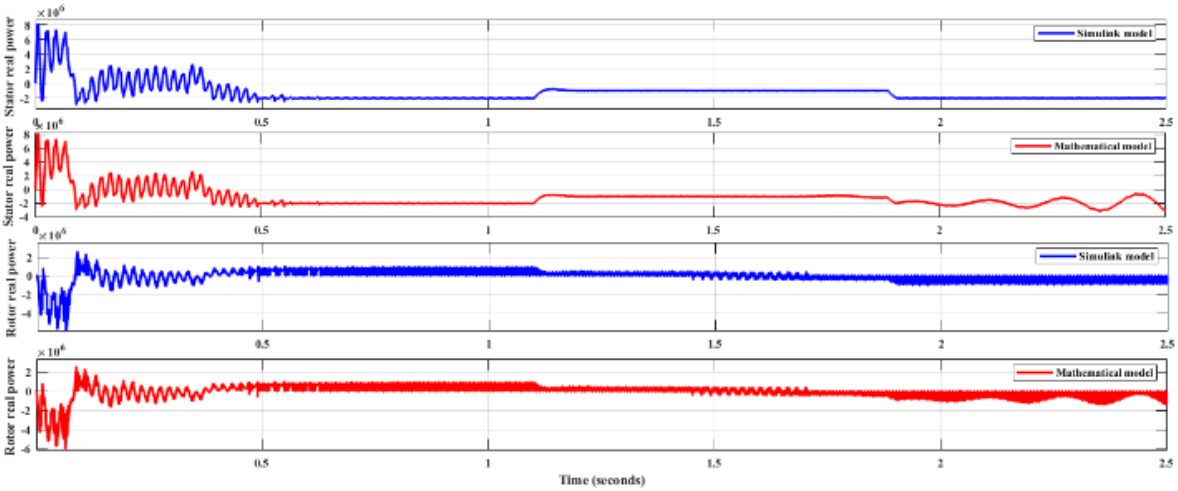

Figure 17. Real power of stator and rotor

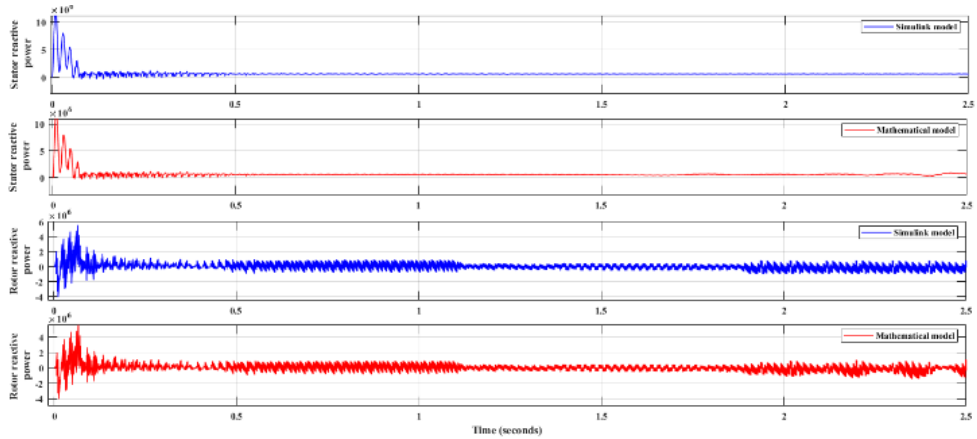

Figure 18. Reactive power of stator and rotor

Figure.18. shows the comparison of reactive power variations resulted from models of both stator and rotor. At a particular operating condition, the whole amount of reactive power (lagging) required for the magnetization of the DFIG needs to be supplied through the stator rather along through the rotor, to have better efficiency. For all operating modes the stator draws the lagging reactive power from the grid and the rotor reactive power is zero.

The comparion in terms of the T_{em} and rotor speed for both models is presented in Figure.19. Till the time 0.5 seconds, electromagnetic torque is in transient state, oscillating with a considerable amount of ripple. After 0.5 seconds steady state is reached, operation below the synchronous speed (1217 rpm) persists till the time 1.20 seconds and the obtained torque, T_{em}

is equal to -12 kNm. Between the time periods 1.20 seconds to 1.89 seconds the machine is operating at synchronous speed and the torque is reduced to -6 kNm, which is half of the rated value. From the time 1.89 to 2.5 seconds, the DFIG is stepped into super-synchronous speed (1800 rpm), in which the generator operates above synchronous speed (T_{em}=-12 kNm). At this mode, mathematical model shows small deviation in steady state compared to Simulink model in the electromagnetic torque as well as the rotor speed response.

Figure.20. shows the comparison results of both models for stator and rotor currents. The DFIG can generate active power to the grid under different operating conditions. As the rotor frequency is slip times supply frequncy (sf_s), it is observed that the rotor frequency is 40Hz when it operates at sub-synchronous speed, 1217rpm. It becomes 0 Hz for the 1500rpm synchronous speed and at the supersynchronous speed, 1800rpm, the rotor frequency is 10Hz. The stator currents indicate the direction of real power flow and the rotor side absorbs real power from the grid in the subsynchronous speed, while it outputs power to the grid in super-synchronous speed. In this state, the mathematical model shows small deviation in steady state compared to Simulink model in both rotor and stator currents.

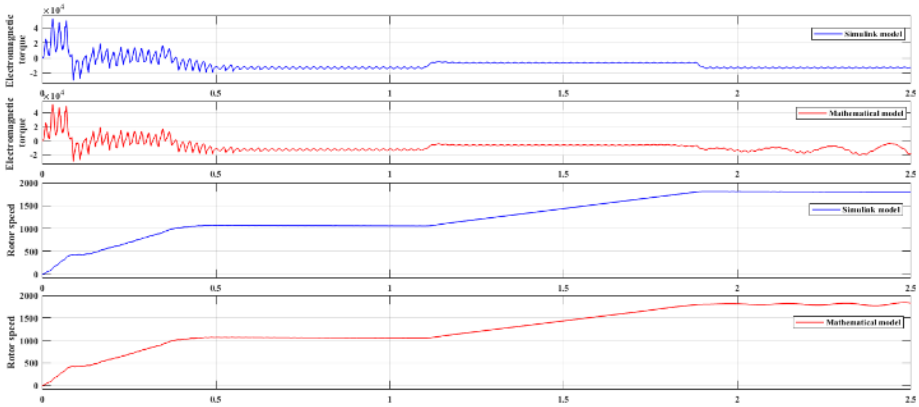

Figure 19. Electromagnetic torque and rotor speed

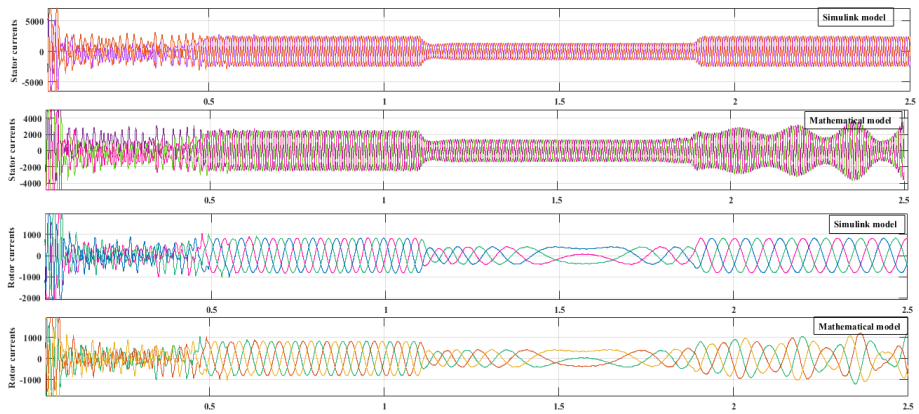

Figure 20. Stator and rotor currents

5. CONCLUSION

The winsome features of doubly fed induction generator based wind energy conversion system have attarcted the researchers vehimently. However, the involved system complexity harderns the further reseacrh, and also the beginers find the ambit very cumbersome. Presenting the simple model and setting up a schematic simulation model can pave the solution to the issue. This paper has described the review of the existing dynamic modeling approaches and state space representations of the doubly fed induction generator based wind energy conversion system, first. The main goal of this analysis is to review the purpose of each model under different operating conditions. Secondly, this paper presents a stator flux oriented vector speed control for the voltage source inverter interfaced doubly fed induction generator while operating with the grid. The performance of the doubly fed induction generator by applying negative electromagnetic torque as input for both mathematical model and Simulink model is analyzed and simulated at standard specifications in MATLAB/Simulink platform. The analysis depicts the behavior of stator and rotor currents, the electromagnetic torque, and the real power and reactive power flow under sub-synchronous speeds, super-synchronous speeds and at synchronous speed of doubly fed induction generator.

REFERENCES

[1] Bull SR. (2001). Renewable energy today and tomorrow. Proceedings of the IEEE 89(8): 1216-1226. http://doi.org/10.1109/5.940290

[2] Kumar Y, Ringenberg J, Depuru SS, Devabhaktuni VK, Lee JW, Nikolaidis E, Andersen B, Afjeh A. (2016).

Wind energy: Trends and enabling technologies. Renewable and Sustainable Energy Reviews 53: 209-224. http://doi.org/10.1016/j.rser.2015.07.200

[3] Guerrero-Rodríguez NF, Rey-Boue AB, Reyes-Archundia E. (2017). Overview and comparative study of two control strategies used in 3-phase grid-connected inverters for renewable systems. Renewable Energy Focus 19-20: 75-89. http://doi.org/10.1016/j.ref.2017.05.007

[4] Chen F, Fu ZG, Yang ZL. (2017). Research on intelligent fault identification technology of wind turbine supported by fault knowledge base. AMSE Journals-AMSE IIETA publication-2017-Series: Modelling A 90(1): 1-15.

[5] Islam MR, Mekhilef S, Saidur R. (2013). Progress and recent trends of wind energy technology. Renewable and Sustainable Energy Reviews 21: 456-468. http://doi.org/10.1016/j.rser.2013.01.007

[6] Blaabjerg F, Ma K. (2017). Wind energy systems. Proceedings of the IEEE 105(11): 2116-2131. http://doi.org/10.1115/1.3267708

[7] Chen Z, Guerrero JM, Blaabjerg F. (2009). A review of the state of the art of power electronics for wind turbines. IEEE Transactions on Power Electronics 24(8): 1859-1875. http://doi.org/10.1109/tpel.2009.2017082

[8] Mohammad SN, Das NK, Roy S. (2014). A review of the state of the art of generators and power electronics for wind energy conversion systems. 3rd International Conference on the Developments in Renewable Energy Technology (ICDRET) 1-6. http://doi.org/10.1109/ICDRET.2014.6861676

[9] Patil NS, Bhosle YN. (2013). A review on wind turbine generator topologies. International Conference in Power. Energy and Control (ICPEC) 625-629. http://doi.org/10.1109/ICPEC.2013.6527733

[10] Soter S, Wegener R. (2007). Development of induction machines in wind power technology. Electric Machines & Drives Conference 2: 1490-1495. http://doi.org/10.1109/IEMDC.2007.383648

[11] Polinder H, Der Pijl FFV, Vilder GJD, Tavner PJ. (2006). Comparison of direct-drive and geared generator concepts for wind turbines. IEEE Transactions on energy conversion 21(3): 725-733. http://doi.org/10.1109/IEMDC.2005.195776

[12] Boroumand JG, Rismanchi B, Saidur R. (2013). Technical characteristic analysis of wind energy conversion systems for sustainable development. Energy conversion and management 69: 87-94. http://doi.org/10.1016/j.enconman.2013.01.030

[13] Ledesma P, Usaola J. (2004). Effect of neglecting stator transients in doubly fed induction generators models. IEEE Transactions on Energy Conversion 19(2): 459-461. http://doi.org/10.1109/tec.2004.827045

[14] Cheng P, Nian H, Wu C, Zhu ZQ. (2017). Direct stator current vector control strategy of DFIG without phase-locked loop during network unbalance. IEEE Transactions on Power Electronics 32(1): 284-297. http://doi.org/10.1109/TPEL.2016.2533638

[15] Wu C, Nian H. (2018). Stator harmonic currents suppression for DFIG based on feed-forward regulator under distorted grid voltage. IEEE Transactions on Power Electronics 33(2): 1211-1224. http://doi.org/10.1109/TPEL.2017.2677527

[16] Zhang Z, Xia CL, Yan Y, Wang HM. (2016). Analytical field calculation of doubly fed induction generator with core saturation considered. 8th IET International Conference on Power Electronics. Machines and Drives (PEMD) 1-6. http://doi.org/10.1049/cp.2016.0130

[17] Soares MN, Gyselinck J, Rolim LGB, Helsen J, Mollet Y. (2018). Loss minimisation strategy for DFIG in wind turbine considering iron losses. IEEE International Conference on Industrial Technology (ICIT) 1025-1030. http://doi.org/10.1109/ICIT.2018.8352319

[18] Balogun A, Ojo O, Okafor F, Karugaba S. (2013). Determination of steady-state and dynamic control laws of doubly fed induction generator using natural and power variables. IEEE Transactions on Industry Applications 49(3): 1343-1357. http://doi.org/10.1109/TIA.2013.2253532

[19] Karakasis N, Mademlis C, Kioskeridis I. (2014). Improved start-up procedure of a stand-alone wind system with doubly-fed induction generator. 7th IET International Conference on Power Electronics, Machines and Drives (PEMD) 1-6. http://doi.org/10.1049/cp.2014.0486

[20] Simon L, Swarup KS. (2016). Impact of DFIG based wind energy conversion system on fault studies and power swings. National Power Systems Conference (NPSC) 1-6. http://doi.org/10.1109/NPSC.2016.7858885

[21] Huerta F, Tello RL, Prodanovic M. (2017). Real-time power-hardware-in-the-loop implementation of variable-speed wind turbines. IEEE Transactions on Industrial Electronics 64(3): 1893-1904. http://doi.org/10.1109/TIE.2016.2624259

[22] Abad G, Lopez J, Rodriguez M, Marroyo L, Iwanski G. (2011). Doubly fed induction machine: modeling and control for wind energy generation. John Wiley & Sons 85: 209-238. http://doi.org/10.1002/9781118104965

[23] Ma J, Qiu Y, Li Y, Zhang W, Song Z, Thorp JS. (2017). Research on the impact of DFIG virtual inertia control on power system small-signal stability considering the phase-locked loop. IEEE Transactions on Power Systems 32(3): 2094-2105. http://doi.org/10.1109/TPWRS.2016.2594781

[24] Fateh F, White WN, Gruenbacher D. (2015). A maximum power tracking technique for grid-connected DFIG-based wind turbines. IEEE Journal of Emerging and Selected Topics in Power Electronics 3(4): 957-966. http://doi.org/10.1109/JESTPE.2015.2448633

[25] Lekube J, Garrido AJ, Garrido I. (2017). Rotational speed optimization in oscillating water column wave power plants based on maximum power point tracking. IEEE Transactions Automation Science and Engineering 14(2): 681-691. http://doi.org/10.1109/TASE.2016.2596579

[26] M'zoughi F, Bouallègue S, Garrido AJ, Garrido I, Ayadi M. (2018). Stalling-free control strategies for oscillating-water-column-based wave power generation plants. IEEE Transactions on Energy Conversion 33(1): 209-222. http://doi.org/10.1109/TEC.2017.2737657

[27] Zou J, Peng C, Xu H, Yan Y. (2015). A fuzzy clustering algorithm-based dynamic equivalent modeling method for wind farm with DFIG. IEEE Transactions on Energy Conversion 30(4): 1329-1337. http://doi.org/10.1109/TEC.2015.2431258

[28] Yu S, Fernando T, Emami K, Iu HHC. (2017). Dynamic state estimation based control strategy for DFIG wind turbine connected to complex power systems. IEEE

Transactions on Power Systems 32(2): 1272-1281. http://doi.org/10.1109/tpwrs.2016.2590951
[29] Huang PH, Moursi MSE, Xia W, Jr JLK. (2013). Novel fault ride-through configuration and transient management scheme for doubly fed induction generator. IEEE Transactions on Energy Conversion 28(1): 86-94. http://doi.org/10.1109/tec.2012.2222886
[30] Ganti VC, Singh B, Aggarwal SK, Kandpal TC. (2012). DFIG-based wind power conversion with grid power leveling for reduced gusts. IEEE Transactions on Sustainable Energy 3(1): 12-20. http://doi.org/10.1109/tste.2011.2170862
[31] Vayeghan MM, Davari SA. (2017). Torque ripple reduction of DFIG by a new and robust predictive torque control method. IET Renewable Power Generation 11(11): 1345-1352. http://doi.org/10.1049/iet-rpg.2016.0695
[32] Zhao H, Lu Z, Huang D, Li Y, Tang H, Tian X, Liu C. (2017). Study on doubly-fed induction generator common model based on transient response characteristics. Chinese Automation Congress (CAC) 7860-7865.
[33] Song Y, Blaabjerg F. (2018). Analysis of Middle Frequency Resonance in DFIG System Considering Phase-Locked Loop. IEEE Transactions on Power Electronics 33(1): 343-356. http://doi.org/10.1109/TPEL.2017.2672867
[34] Abdelbaset A, El-Sayed AHM, Abozeid AEH. (2017). Grid synchronisation enhancement of a wind driven DFIG using adaptive sliding mode control. IET Renewable Power Generation 11(5): 688-695. http://doi.org/10.1049/iet-rpg.2016.0392
[35] Sun D, Wang X, Nian H, Zhu ZQ. (2018). A sliding-mode direct power control strategy for DFIG under both balanced and unbalanced grid conditions using extended active power. IEEE Transactions on Power Electronics 33(2): 1313-1322. http://doi.org/10.1109/TPEL.2017.2686980
[36] Wang T, Nian H, Zhu Z. (2017). Flexible unbalance compensation strategy for doubly fed induction generator based on a novel indirect virtual impedance method. IET Renewable Power Generation 12(1): 28-36. http://doi.org/10.1049/iet-rpg.2016.0923

NOMENCLATURE AND ABBREVIATIONS

v_{as}, v_{bs}, v_{cs} ; v_{ar}, v_{br}, v_{cr}	Stator voltages and rotor voltages in abc axis
i_{as}, i_{bs}, i_{cs} ; i_{ar}, i_{br}, i_{cr}	Stator currents and rotor currents in abc axis
$\psi_{as}, \psi_{bs}, \psi_{cs}; \psi_{ar}, \psi_{br}, \psi_{cr}$	Flux linkages of stator and rotor in abc axis
$i_{\alpha s}, i_{\beta s}, i_{\alpha r}\ i_{\beta r}$	Stator currents and rotor currents in $\alpha\beta$ axis
$V_{\alpha s}, V_{\beta s}, V_{\alpha r}, V_{\beta r}$	Voltages w.r.t stator and rotor in $\alpha\beta$ axis
$i_{ds}, i_{qs}, i_{dr}, i_{qs}$	Currents w.r.t stator and rotor in dq axis
$V_{ds}, V_{qs}, V_{dr}, V_{qs}$	Voltages w.r.t stator and rotor in dq axis
R_s, R_r	Stator resistance and rotor resistance
L_s, L_r, L_m	Inductances w.r.t stator, rotor and magnetization
$L_{\sigma s}, L_{\sigma r}$	Leakage inductances of stator and rotor
ω_s, ω_r	Angular frequency of stator and angular frequency of rotor
ω_m, Ω_m	Electrical and mechanical angular frequencies
p	Pole pairs
σ	Leakage factor
WECS	Wind energy conversion system
WPGS	Wind power generation system
DFIG	Doubly fed induction generator
SRRF	Synchronous rotating reference frame
RRF	Rotor reference frame
SRF	Stator reference frame
IG	Induction generator
SC	Squirrel cage
WF	Wound field
DF	Doubly fed
SG	Synchronous generator
PM	Permanent magnet
TIVS	Time invariant system
TVS	Time variant system
VC	Vector control
BEMF	Back electromotive force
DSPs	Digital signal processor
FPGAs	Field programmable gate arrays
TF	Transfer function